Abf1	Abf2	Ace2	Adr1	Aft1	Aft2
Aro80	Asg1	Azf1	Bas1	Cad1	Cat8
Cbf1	Cep3	Cha4	Cin5	Crz1	Cst6
Cup9	Dal80	Dal82	Ecm22	Ecm23	Fhl1
Fkh1	Fkh2	Fzf1	Gal4	Gat1	Gat3
Gat4	Gcn4	Gcr1	Gis1	Gln3	Gsm1
Gzf3	Hac1	Hal9	Hap1	Hcm1	Hmlalpha2
Hmra2	Hsf1	Leu3	Lys14	Matalpha2	Mbp1
Mcm1	Met31	Met32	Mga1	Mig1	Mig2
Mig3	Mot3	Msn1	Msn2	Msn4	Ndt80
Nhp10	Nhp6a	Nhp6b	Nrg1	Nrg2	Oaf1
Pbf1	Pbf2	Pdr1	Pdr3	Phd1	Pdr8
Pho2	Pho4	Put3	Rap1	Rdr1	Rds1
Rds2	Reb1	Rei1	Rfx1	Rgm1	Rgt1
Rim101	Rox1	Rph1	Rpn4	Rsc3	Rsc30
Rtg3	Sfl1	Sfp1	Sig1	Sip4	Skn7
Sko1	Smp1	Sok2	Spt15	Srd1	Stb3
Stb4	Stb5	Ste12	Stp1	Stp2	Stp3
Stp4	Sum1	Sut1	Sut2	Swi4	Swi5
Tbf1	Tbs1	Tea1	Tec1	Tos8	Tye7
Uga3	Ume6	Upc2	Usv1	Vhr1	Xbp1
Yap1	Yap3	Yap6	YBR033W	YBR239C	YDR520C
YER064C	YER130C	YER184C	YGR067C	YKL222C	YLL054C
YLR278C	YML081W	YNR063W	Yox1	YPR013C	YPR015C
YPR022C	YPR196W	Yrm1	Yrr1	Zap1	Zms1

Table S1: List of 150 TFs used by RoboCOP. All TFs excepting the ones colored in gray have binding sites reported in MacIsaac *et al.* (2006). The TFs colored in red have alternate validation sets from ChIP-exo (Rhee and Pugh, 2011) and ORGANIC (Kasinathan *et al.*, 2014) protocols. The ones colored in blue are known to express more under specific experimental conditions (Harbison *et al.*, 2004).

top100	**bottom100**	**mid100**
HXK1	RPL9A	TCM62
HSP78	RPS22A	MCK1
MMP1	SSB1	AGC1
YHR138C	RPS31	GPB2
YET1	RPS3	HEH2
HNT1	ASC1	YPL168W
GOR1	RPL3	MRK1
STF1	YEF3	SEN2
HOM6	RPL8B	MTC2
MET8	RPS9B	FCY21
PRC1	RPL5	CDD1
GSC2	RPS5	CDC24
PGM2	RPP2B	COX11
GSH1	RPS12	TFC8
YER067W	RPL12A	IME1
CPR1	RPS2	YBP1
RTS3	RPP2A	YEL1
ARN2	RPP0	IST3
WTM1	RPP1A	PKC1
MET22	RPS15	DTD1
GPM1	RPS0B	ADY4
DDR2	RPL28	VPS52
HOR7	RPL38	YGR153W
MUP1	RPS14A	YPL199C
GPD1	ILV5	FRT1
GRE2	RPL16B	LEM3
ARA1	RPL22A	PFA3
SER33	RPL2A	CUE2
YLR194C	RPL1B	PSY3
ENO1	RPL2B	THI72
CMK2	RPL32	SHU2
GRX1	SSB2	NSP1
ALD4	RPL1A	RAD53
GSP2	RPS16B	YKL065W-A
MUP3	RPL18A	RAD24
YOR285W	RPL25	ATG16
MET2	RPS13	VRP1
FMO1	RPL11A	MLH2
MRP8	RPL21A	MSY1
YBR085C-A	RPL26B	ADE2
TRX2	RPL17A	BTS1
SAM2	RPL15A	EXO84
PDI1	RPL30	YNL165W
MXR1	RPS11A	ASF2
TFS1	RPS8A	IOC2
TPS1	RPS1B	MNT3
YMR315W	RPS4A	CBF1 *(contd.)*

top100	bottom100	mid100
PRX1	RPS26B	CSN12
ERO1	RPL19B	AYT1
TSL1	RPL31A	MSS11
HSP82	RPS7A	KIP1
PGK1	SNU13	CCT3
GRE3	RPS4B	EAF6
YNL134C	RPS20	PUS5
AIM17	RPL42B	DSS1
SSA1	RPL27A	RPB11
MET1	RPS18B	YNL176C
GLK1	RPS0A	NTE1
FIT2	RPL12B	SGF73
HBN1	RPS10A	PRK1
TDH1	RPL13B	TRR1
HSP104	RPL6B	APC5
AGP3	RPL8A	HOS2
FIT3	RPL24A	MSE1
SEO1	NSR1	QDR1
MET6	RPS24B	MTC5
YNL208W	RPS18A	YIR035C
PHO89	RPS6B	GLE1
ICY2	RPL11B	RTT103
MET16	RPS6A	MNS1
LAP4	RPL6A	NHP10
PEP4	RPL20A	FTR1
TSA1	RPS24A	FLC1
UBI4	RPL43A	RTC5
HSP42	RPS8B	PLB3
BNA3	RPL33A	PAU15
KAR2	NOP1	FIT1
TIS11	RPL4A	BIO3
RTC3	RPL14A	CTK3
TMA10	RPS19B	AIM33
ZWF1	TMA19	MMS21
PBI2	RPL16A	YLR253W
BDS1	RPL37A	LRC6
YCT1	RPL19A	ISC1
PNC1	RPL7A	SGM1
CYS3	RPS17A	RSM28
PRB1	RPL17B	RRP43
ECM17	RPS23B	CFT2
SPG4	RPS27B	YMR166C
GRE1	RPL20B	GYL1
STF2	RPS11B	NUP49
MET10	RPL23A	GGA2
AHP1	RPS28A	YPL257W
DDR48	STM1	MEC1
MET14	RPL40B	SMP3
HSP26	RPL34B	EAP1
YDL124W	RPP1B	CDC11
PDC6	RPL39	CDC26
MET3	ILV3	SAG1
HSP12	RPL23B	YHC1

Table S2: List of 100 most upregulated, most downregulated genes. And 100 genes with almost no changes in transcription.

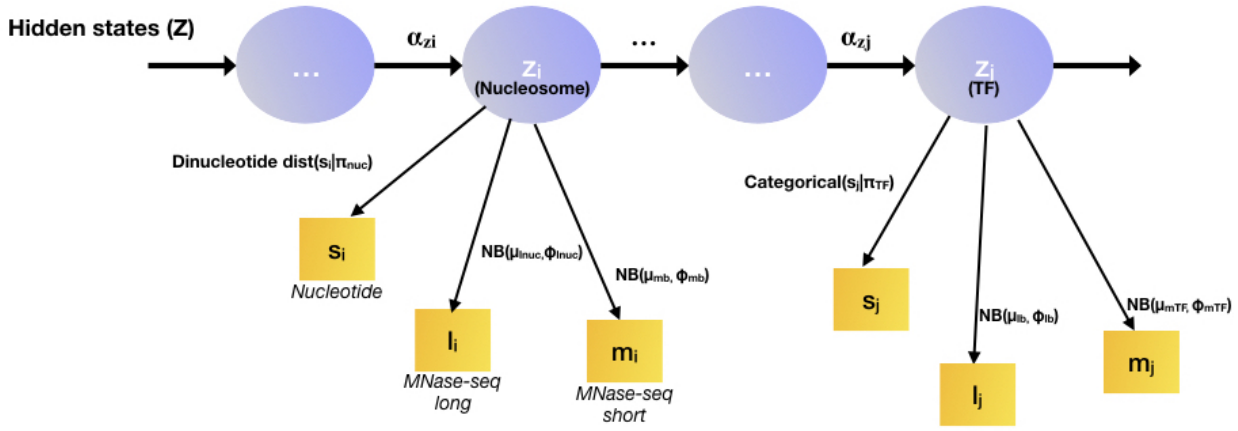

Figure S1: Hidden state sequence of RoboCOP. Each state emits a nucleotide using a categorical distribution, number of midpoints of nucFrags using a negative binomial distribution, and number of midpoints of shortFrags using a negative binomial distribution.

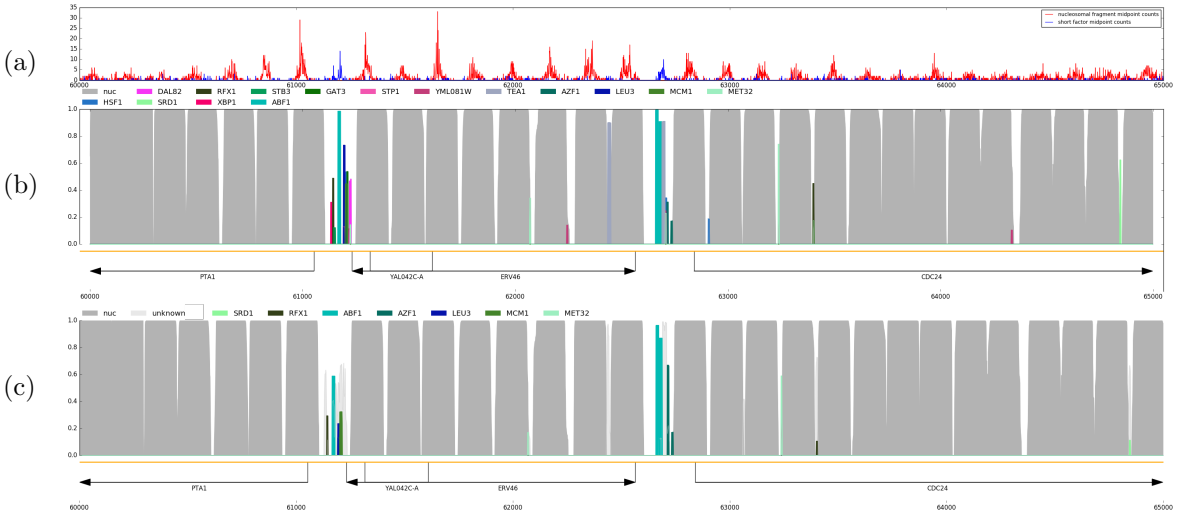

Figure S2: (a) MNase-seq fragment midpoint counts. Running RoboCOP (b) with and (c) without "unknown" factor. In (c) we observe more clustering of TFs means there are more false positives. Adding "unknown" factor as DBF reduces TF clustering thereby reducing number of false positive predictions.

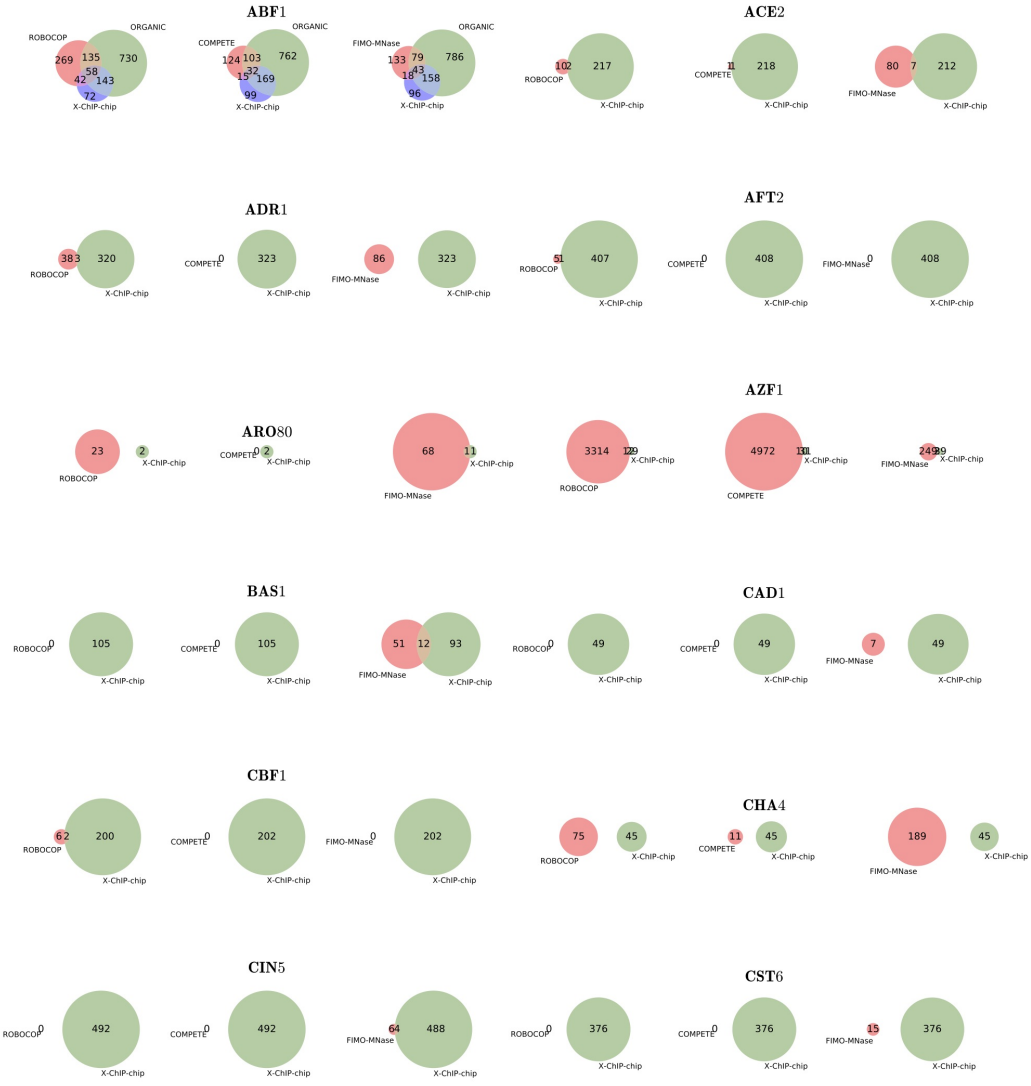
ABF1
ROBOCOP
ORGANIC
X-ChIP-chip
269
135
730
58
42
143
72
COMPETE
ORGANIC
X-ChIP-chip
124
103
762
32
15
169
99
FIMO-MNase
ORGANIC
X-ChIP-chip
133
79
786
43
18
158
96
ACE2
ROBOCOP
X-ChIP-chip
102
217
COMPETE
X-ChIP-chip
11
218
FIMO-MNase
X-ChIP-chip
80
7
212
ADR1
ROBOCOP
X-ChIP-chip
383
320
COMPETE
X-ChIP-chip
0
323
FIMO-MNase
X-ChIP-chip
86
323
AFT2
ROBOCOP
X-ChIP-chip
51
407
COMPETE
X-ChIP-chip
0
408
FIMO-MNase
X-ChIP-chip
0
408
AZF1
ROBOCOP
X-ChIP-chip
23
2
ARO80
COMPETE
X-ChIP-chip
0
2
FIMO-MNase
X-ChIP-chip
68
11
ROBOCOP
X-ChIP-chip
3314
129
COMPETE
X-ChIP-chip
4972
131
FIMO-MNase
X-ChIP-chip
249
29
BAS1
ROBOCOP
X-ChIP-chip
0
105
COMPETE
X-ChIP-chip
0
105
FIMO-MNase
X-ChIP-chip
51
12
93
CAD1
ROBOCOP
X-ChIP-chip
0
49
COMPETE
X-ChIP-chip
0
49
FIMO-MNase
X-ChIP-chip
7
49
CBF1
ROBOCOP
X-ChIP-chip
62
200
COMPETE
X-ChIP-chip
0
202
FIMO-MNase
X-ChIP-chip
0
202
CHA4
ROBOCOP
X-ChIP-chip
75
45
COMPETE
X-ChIP-chip
11
45
FIMO-MNase
X-ChIP-chip
189
45
CIN5
ROBOCOP
X-ChIP-chip
0
492
COMPETE
X-ChIP-chip
0
492
FIMO-MNase
X-ChIP-chip
64
488
CST6
ROBOCOP
X-ChIP-chip
0
376
COMPETE
X-ChIP-chip
0
376
FIMO-MNase
X-ChIP-chip
15
376

DAL80
ROBOCOP 0
303
X-ChIP-chip
COMPETE 0
303
X-ChIP-chip
FIMO-MNase 12
303
X-ChIP-chip
DAL82
64 5
340
ROBOCOP
X-ChIP-chip
COMPETE 12
345
X-ChIP-chip
143 9
336
FIMO-MNase
X-ChIP-chip
FHL1
ROBOCOP 7
207
X-ChIP-chip
COMPETE 0
207
X-ChIP-chip
74
FIMO-MNase
207
X-ChIP-chip
FKH1
ROBOCOP 0
338
X-ChIP-chip
COMPETE 0
338
X-ChIP-chip
145
FIMO-MNase
333
X-ChIP-chip
FKH2
41 20
302
ROBOCOP
X-ChIP-chip
124
COMPETE
318
X-ChIP-chip
108
FIMO-MNase
314
X-ChIP-chip
GAL4
319 126
X-ChIP-chip
ROBOCOP
102 612
X-ChIP-chip
COMPETE
152 126
X-ChIP-chip
FIMO-MNase
GAT1
ROBOCOP 0
142
X-ChIP-chip
COMPETE 0
142
X-ChIP-chip
24 1
FIMO-MNase
141
X-ChIP-chip
GAT3
ROBOCOP 0
112
X-ChIP-chip
COMPETE 0
112
X-ChIP-chip
14
FIMO-MNase
112
X-ChIP-chip
GCN4
ROBOCOP 0
318
X-ChIP-chip
COMPETE 0
318
X-ChIP-chip
49
FIMO-MNase
309
X-ChIP-chip
GCR1
288 9 68
X-ChIP-chip
ROBOCOP
220 2 75
X-ChIP-chip
COMPETE
58 6 71
FIMO-MNase
X-ChIP-chip
GLN3
ROBOCOP 1
412
X-ChIP-chip
COMPETE 0
412
X-ChIP-chip
FIMO-MNase 0
412
X-ChIP-chip
GZF3
ROBOCOP 0
80
X-ChIP-chip
COMPETE 0
80
X-ChIP-chip
15 1
79
FIMO-MNase
X-ChIP-chip

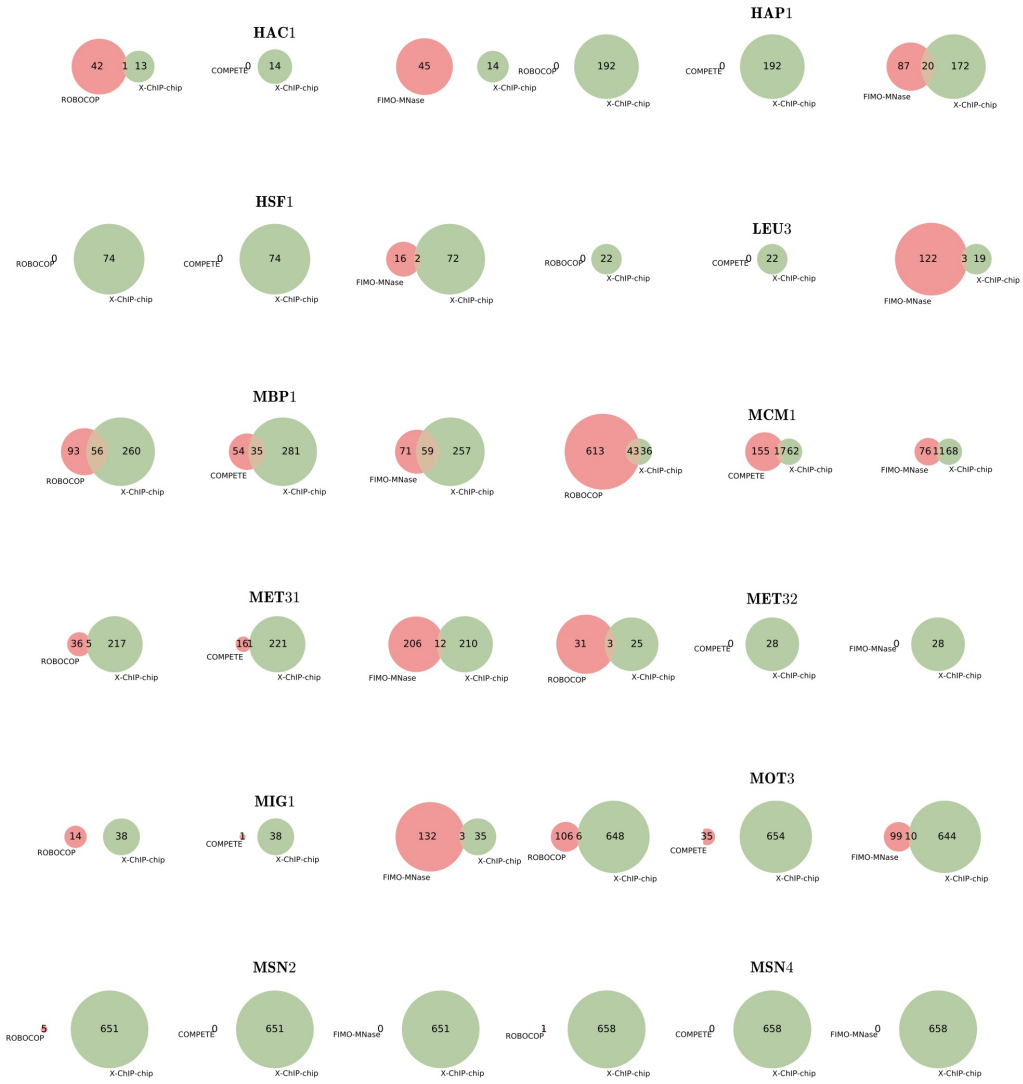
HAC1
42
1
13
ROBOCOP
X-ChIP-chip
0
14
COMPETE
X-ChIP-chip
45
14
FIMO-MNase
X-ChIP-chip
0
192
ROBOCOP
X-ChIP-chip
HAP1
0
192
COMPETE
X-ChIP-chip
87
20
172
FIMO-MNase
X-ChIP-chip
HSF1
0
74
ROBOCOP
X-ChIP-chip
0
74
COMPETE
X-ChIP-chip
16
2
72
FIMO-MNase
X-ChIP-chip
0
22
ROBOCOP
X-ChIP-chip
LEU3
0
22
COMPETE
X-ChIP-chip
122
3
19
FIMO-MNase
X-ChIP-chip
MBP1
93
56
260
ROBOCOP
X-ChIP-chip
54
35
281
COMPETE
X-ChIP-chip
71
59
257
FIMO-MNase
X-ChIP-chip
613
4336
X-ChIP-chip
ROBOCOP
MCM1
155
1762
COMPETE
X-ChIP-chip
76
1168
FIMO-MNase
X-ChIP-chip
MET31
36
5
217
ROBOCOP
X-ChIP-chip
161
221
COMPETE
X-ChIP-chip
206
12
210
FIMO-MNase
X-ChIP-chip
31
3
25
ROBOCOP
X-ChIP-chip
MET32
0
28
COMPETE
X-ChIP-chip
0
28
FIMO-MNase
X-ChIP-chip
MIG1
14
38
ROBOCOP
X-ChIP-chip
1
38
COMPETE
X-ChIP-chip
132
3
35
FIMO-MNase
X-ChIP-chip
106
6
648
ROBOCOP
X-ChIP-chip
MOT3
35
654
COMPETE
X-ChIP-chip
99
10
644
FIMO-MNase
X-ChIP-chip
MSN2
5
651
ROBOCOP
X-ChIP-chip
0
651
COMPETE
X-ChIP-chip
0
651
FIMO-MNase
X-ChIP-chip
1
658
ROBOCOP
X-ChIP-chip
MSN4
0
658
COMPETE
X-ChIP-chip
0
658
FIMO-MNase
X-ChIP-chip

NRG1
ROBOCOP
31
281
X-ChIP-chip
COMPETE
0
282
X-ChIP-chip
FIMO-MNase
51
34
248
X-ChIP-chip
PDR1
ROBOCOP
1
42
X-ChIP-chip
COMPETE
0
42
X-ChIP-chip
FIMO-MNase
154
42
X-ChIP-chip
PDR3
ROBOCOP
77
20
X-ChIP-chip
COMPETE
70
20
X-ChIP-chip
FIMO-MNase
141
20
X-ChIP-chip
PHD1
ROBOCOP
0
1208
X-ChIP-chip
COMPETE
0
1209
X-ChIP-chip
FIMO-MNase
464
1205
X-ChIP-chip
PHO2
ROBOCOP
0
2180
X-ChIP-chip
COMPETE
0
2180
X-ChIP-chip
FIMO-MNase
5
2180
X-ChIP-chip
PHO4
ROBOCOP
0
46
X-ChIP-chip
COMPETE
0
46
X-ChIP-chip
FIMO-MNase
34
9
37
X-ChIP-chip
PUT3
ROBOCOP
3
6
X-ChIP-chip
COMPETE
0
6
X-ChIP-chip
FIMO-MNase
204
6
X-ChIP-chip
RAP1
ROBOCOP
ChIP-exo
338
156
261
111
43
32
97
X-ChIP-chip
COMPETE
ChIP-exo
258
122
295
90
41
53
98
X-ChIP-chip
FIMO-MNase
ChIP-exo
170
108
309
70
8
73
132
X-ChIP-chip
RDS1
ROBOCOP
10
1
17
X-ChIP-chip
COMPETE
0
1
17
X-ChIP-chip
FIMO-MNase
130
10
8
X-ChIP-chip
REB1
ROBOCOP
ChIP-exo
91
32
486
63
400
506
974
ORGANIC
COMPETE
ChIP-exo
98
30
488
116
418
488
921
ORGANIC
FIMO-MNase
ChIP-exo
12
7
500
17
148
759
1020
ORGANIC
RFX1
ROBOCOP
1
15
X-ChIP-chip
COMPETE
0
15
X-ChIP-chip
FIMO-MNase
28
1
14
X-ChIP-chip
ROBOCOP
281
111
X-ChIP-chip
RGT1
COMPETE
0
12
X-ChIP-chip
FIMO-MNase
196
39
X-ChIP-chip

RIM101
98
ROBOCOP
11
X-ChIP-chip
COMPETE 0
11
X-ChIP-chip
86
FIMO-MNase
11
X-ChIP-chip
ROBOCOP 0
380
X-ChIP-chip
ROX1
COMPETE 0
380
X-ChIP-chip
FIMO-MNase 0
380
X-ChIP-chip
ROBOCOP 0
RPH1
3
X-ChIP-chip
COMPETE 0
3
X-ChIP-chip
RPN4
41
FIMO-MNase
3
X-ChIP-chip
86
2
95
ROBOCOP
X-ChIP-chip
101
COMPETE
96
X-ChIP-chip
139
28
69
FIMO-MNase
X-ChIP-chip
RTG3
28
ROBOCOP
321
X-ChIP-chip
COMPETE 0
321
X-ChIP-chip
94
2
319
FIMO-MNase
X-ChIP-chip
SFP1
1442
ROBOCOP
110
X-ChIP-chip
1136
COMPETE
110
X-ChIP-chip
189
FIMO-MNase
110
X-ChIP-chip
SIP4
ROBOCOP 0
10
X-ChIP-chip
COMPETE 0
10
X-ChIP-chip
102
FIMO-MNase
10
X-ChIP-chip
314
ROBOCOP
479
X-ChIP-chip
SKN7
COMPETE 0
483
X-ChIP-chip
66
19
464
FIMO-MNase
X-ChIP-chip
SKO1
ROBOCOP 0
88
X-ChIP-chip
COMPETE 0
88
X-ChIP-chip
23
5
83
FIMO-MNase
X-ChIP-chip
3
ROBOCOP
3
X-ChIP-chip
SMP1
COMPETE 0
3
X-ChIP-chip
3
FIMO-MNase
3
X-ChIP-chip
SOK2
119
2
801
ROBOCOP
X-ChIP-chip
22
COMPETE
803
X-ChIP-chip
517
FIMO-MNase
796
X-ChIP-chip
STB4
ROBOCOP 0
11
X-ChIP-chip
COMPETE 0
11
X-ChIP-chip
63
3
8
X-ChIP-chip
FIMO-MNase

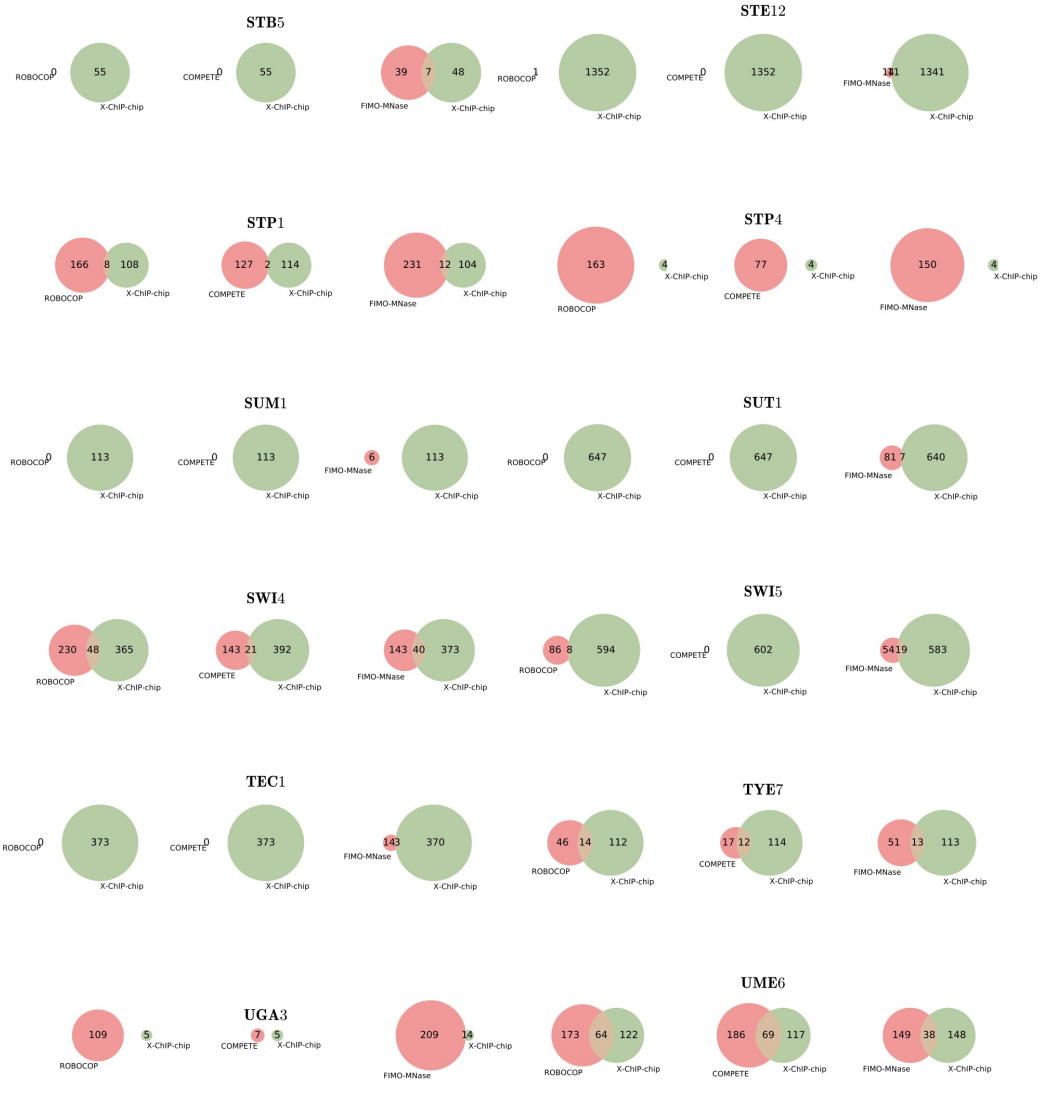
STB5
ROBOCOP
0
55
X-ChIP-chip
COMPETE
0
55
X-ChIP-chip
FIMO-MNase
39
7
48
X-ChIP-chip
STE12
ROBOCOP
1
1352
X-ChIP-chip
COMPETE
0
1352
X-ChIP-chip
FIMO-MNase
1
1341
X-ChIP-chip
STP1
166
8
108
ROBOCOP
X-ChIP-chip
127
2
114
COMPETE
X-ChIP-chip
231
12
104
FIMO-MNase
X-ChIP-chip
STP4
163
ROBOCOP
4
X-ChIP-chip
77
COMPETE
4
X-ChIP-chip
150
FIMO-MNase
4
X-ChIP-chip
SUM1
ROBOCOP
0
113
X-ChIP-chip
COMPETE
0
113
X-ChIP-chip
FIMO-MNase
6
113
X-ChIP-chip
SUT1
ROBOCOP
0
647
X-ChIP-chip
COMPETE
0
647
X-ChIP-chip
FIMO-MNase
81
7
640
X-ChIP-chip
SWI4
230
48
365
ROBOCOP
X-ChIP-chip
143
21
392
COMPETE
X-ChIP-chip
143
40
373
FIMO-MNase
X-ChIP-chip
SWI5
86
8
594
ROBOCOP
X-ChIP-chip
COMPETE
0
602
X-ChIP-chip
54
19
583
FIMO-MNase
X-ChIP-chip
TEC1
ROBOCOP
0
373
X-ChIP-chip
COMPETE
0
373
X-ChIP-chip
FIMO-MNase
143
370
X-ChIP-chip
TYE7
46
14
112
ROBOCOP
X-ChIP-chip
17
12
114
COMPETE
X-ChIP-chip
51
13
113
FIMO-MNase
X-ChIP-chip
UGA3
109
ROBOCOP
5
X-ChIP-chip
COMPETE
7
5
X-ChIP-chip
209
14
FIMO-MNase
X-ChIP-chip
UME6
173
64
122
ROBOCOP
X-ChIP-chip
186
69
117
COMPETE
X-ChIP-chip
149
38
148
FIMO-MNase
X-ChIP-chip

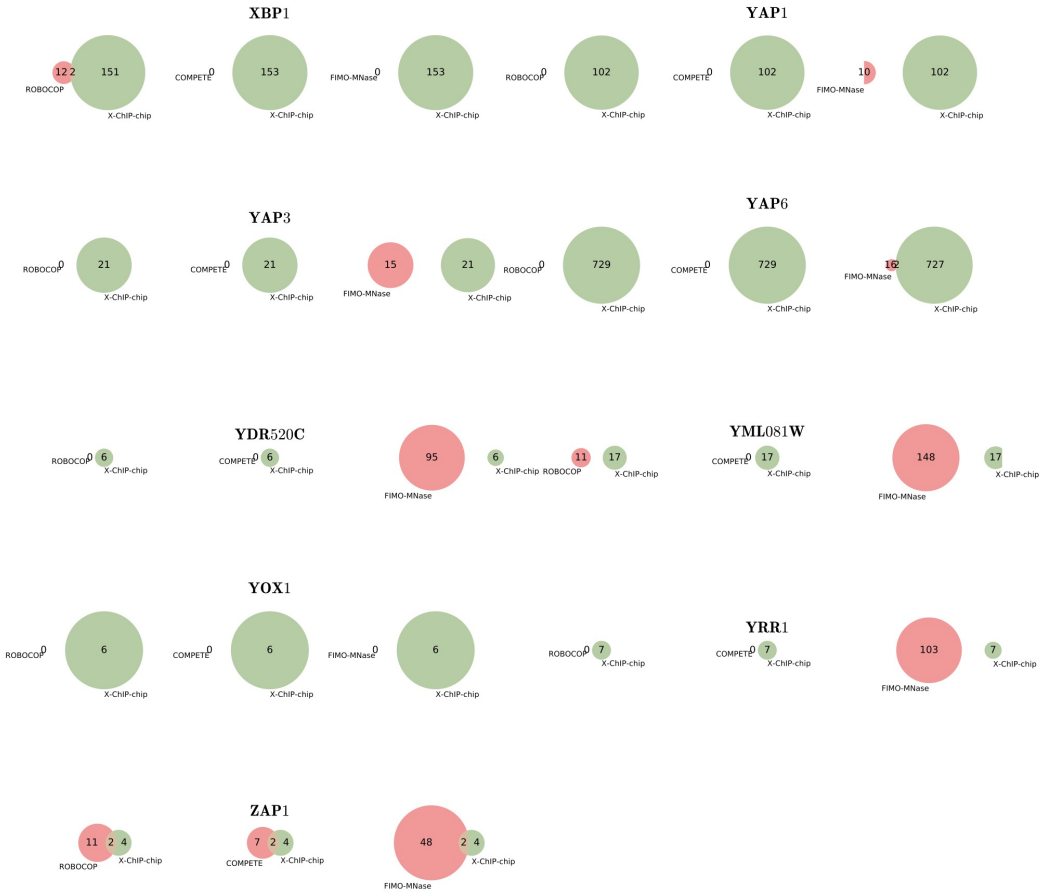

Figure S3: Venn digrams comparing the TF binding site predictions of RoboCOP, COMPETE, and FIMO-MNase with reported binding sites from X-ChIP-chip (MacIsaac *et al.*, 2006), ChIP-exo (Rhee and Pugh, 2011) and ORGANIC (Kasinathan *et al.*, 2014).

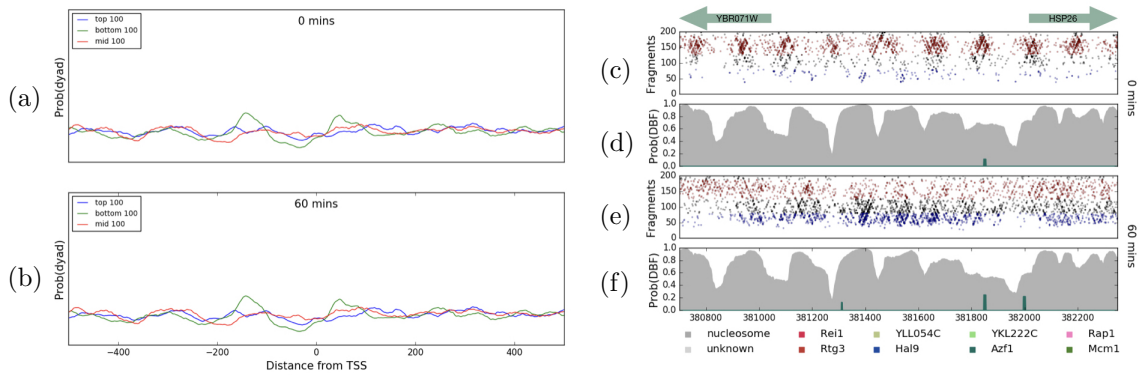

Figure S4: Aggregate of P(dyad) computed by COMPETE around the TSS of genes that are most up-regulated (blue), most down-regulated (green) and no change in transcription (red) (a) before, and (b) after treating cells with cadmium. We find that COMPETE is unable to capture the chromatin dynamics around the TSS. MNase-seq midpoint plot and COMPETE predicted binding landscape of HSP26 promoter at chrII:380700-382350 (c) before and (e) after treatment with cadmium. As MNase-seq is not an input to COMPETE, it fails to capture the changes in chromatin under cadmium treatment.

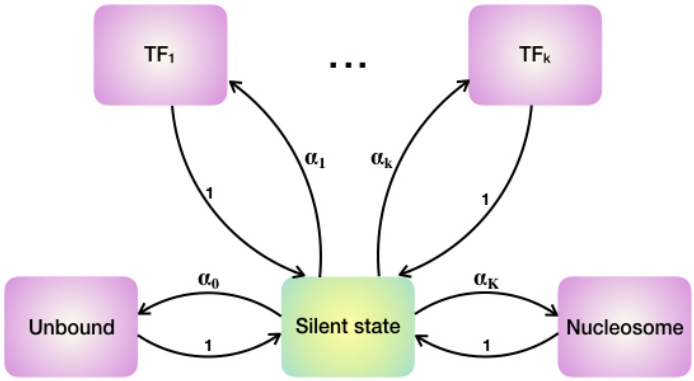

Figure S5: Transition diagram among the different DBFs. The DBFs are nucleosome, TFs and unbound state. The model transitions to a DBF k with probability α_k and then comes back to the silent state with a probability of 1.

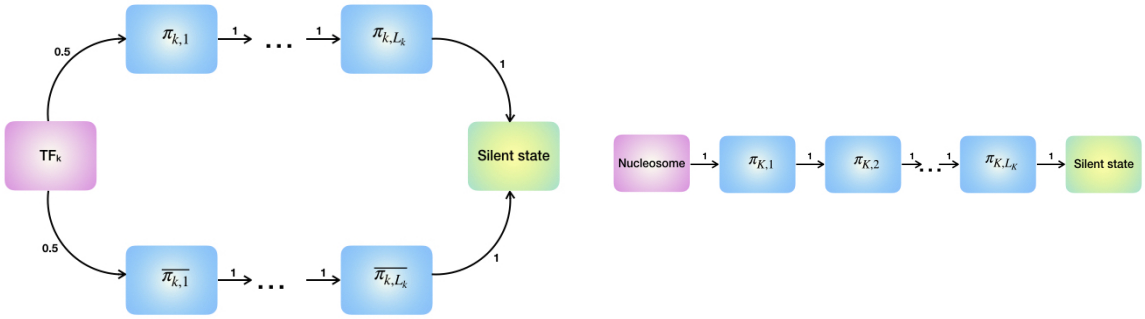

Figure S6: (a) State transition diagram of a TF. The model puts equal weight to transition into the motif and the reverse complement of the motif. After transitioning through the entire motif, it transitions back to the central silent state with probability of 1. (b) State transition diagram of the nucleosome model. Nucleosomes are modeled to be 147 bases long. After transitioning through the 147 nucleosome states the model transitions back to the central silent state.

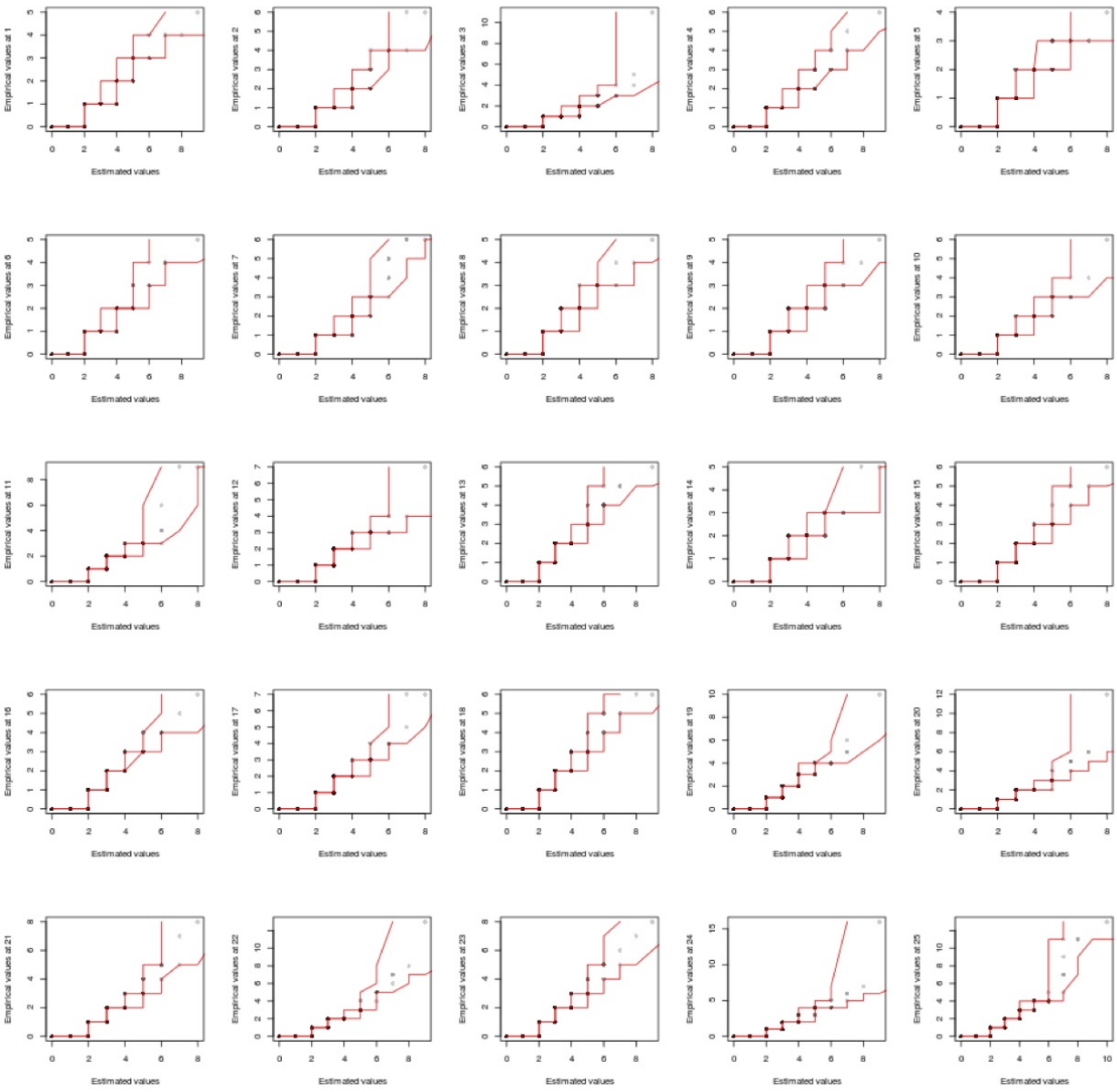
Empirical values at 1
Empirical values at 2
Empirical values at 3
Empirical values at 4
Empirical values at 5
Empirical values at 6
Empirical values at 7
Empirical values at 8
Empirical values at 9
Empirical values at 10
Empirical values at 11
Empirical values at 12
Empirical values at 13
Empirical values at 14
Empirical values at 15
Empirical values at 16
Empirical values at 17
Empirical values at 18
Empirical values at 19
Empirical values at 20
Empirical values at 21
Empirical values at 22
Empirical values at 23
Empirical values at 24
Empirical values at 25
Estimated values

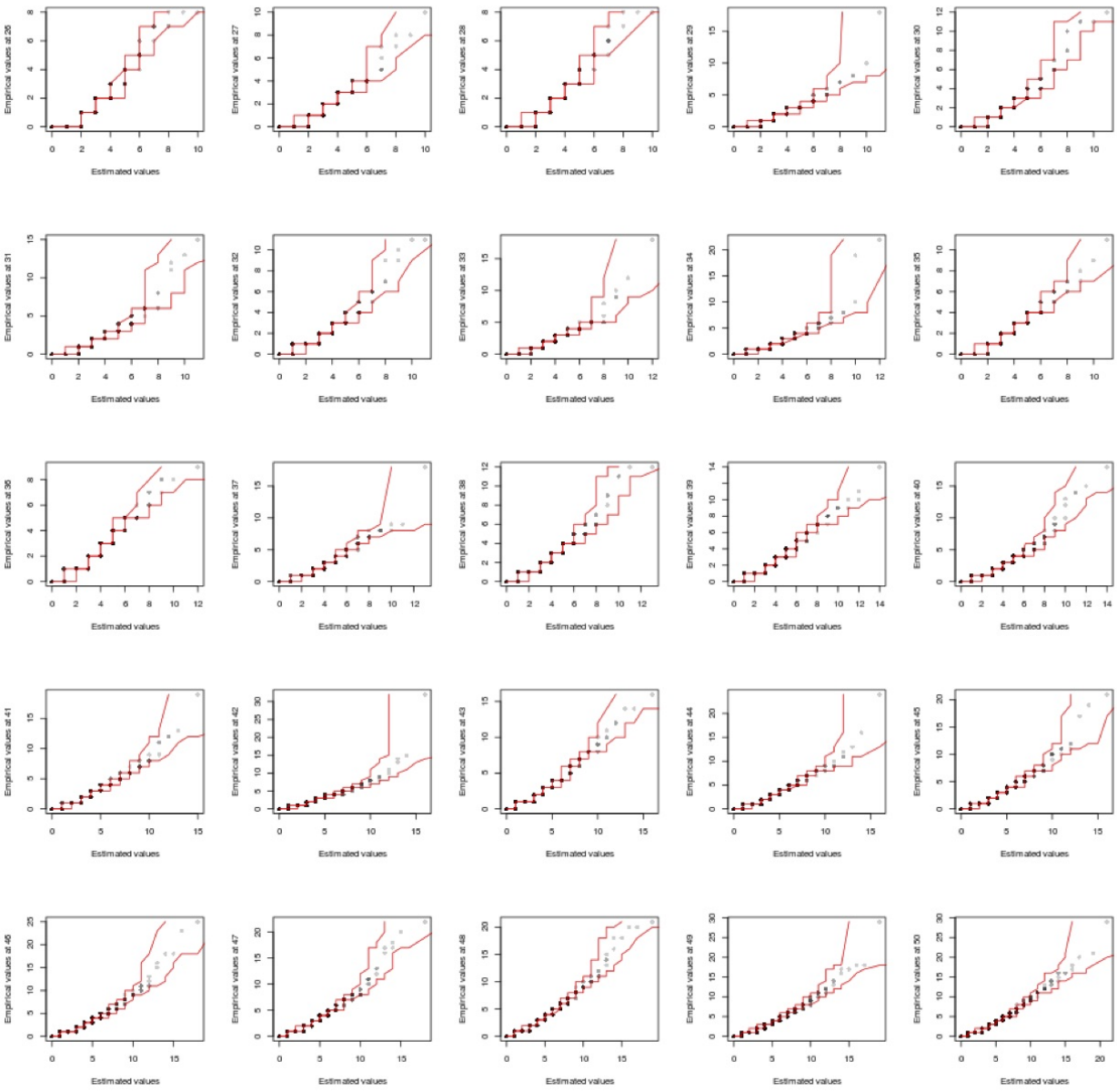
Empirical values at 26
Empirical values at 27
Empirical values at 28
Empirical values at 29
Empirical values at 30
Empirical values at 31
Empirical values at 32
Empirical values at 33
Empirical values at 34
Empirical values at 35
Empirical values at 36
Empirical values at 37
Empirical values at 38
Empirical values at 39
Empirical values at 40
Empirical values at 41
Empirical values at 42
Empirical values at 43
Empirical values at 44
Empirical values at 45
Empirical values at 46
Empirical values at 47
Empirical values at 48
Empirical values at 49
Empirical values at 50
Estimated values

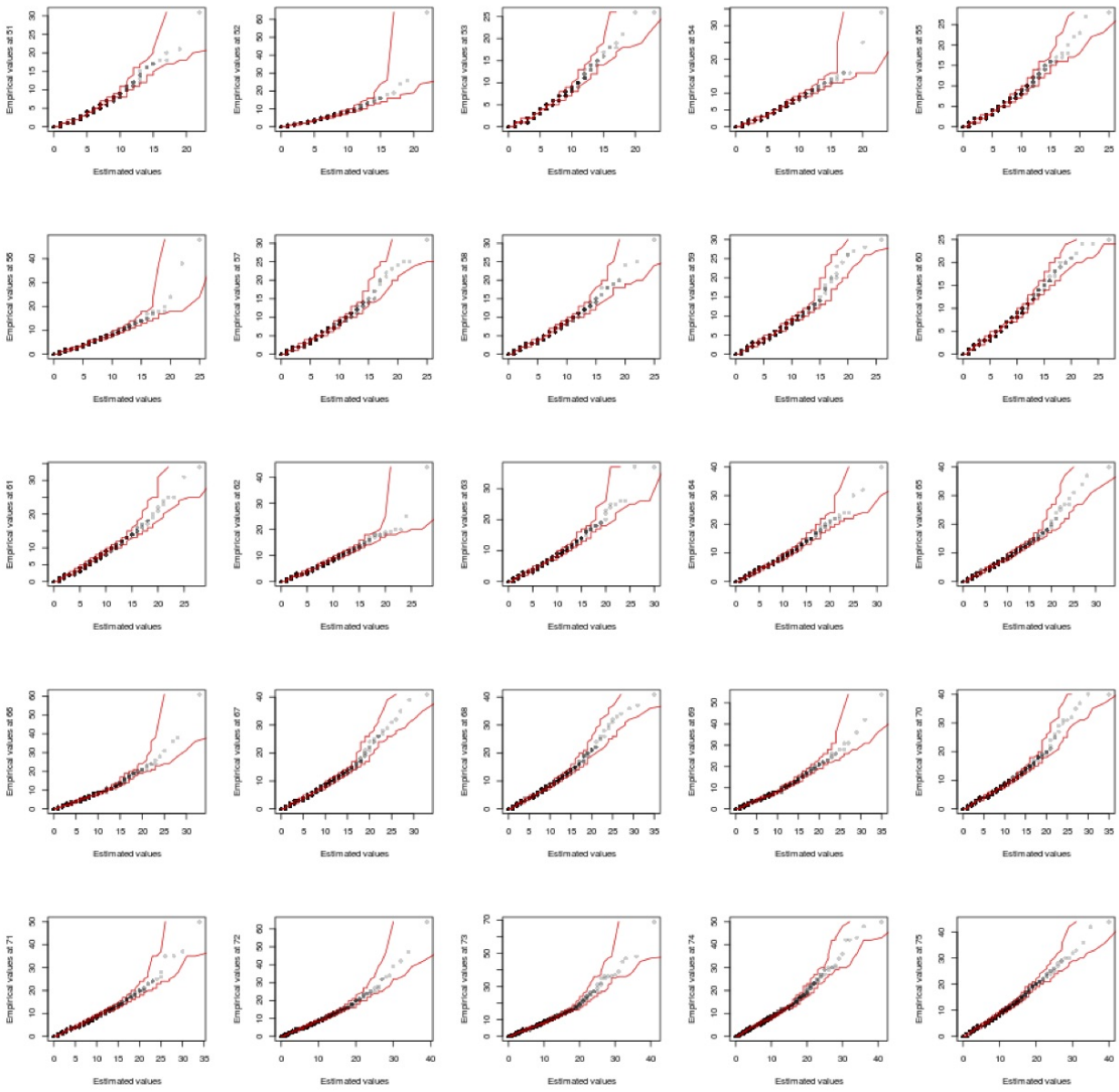
Empirical values at 51
Empirical values at 52
Empirical values at 53
Empirical values at 54
Empirical values at 55
Empirical values at 56
Empirical values at 57
Empirical values at 58
Empirical values at 59
Empirical values at 60
Empirical values at 61
Empirical values at 62
Empirical values at 63
Empirical values at 64
Empirical values at 65
Empirical values at 66
Empirical values at 67
Empirical values at 68
Empirical values at 69
Empirical values at 70
Empirical values at 71
Empirical values at 72
Empirical values at 73
Empirical values at 74
Empirical values at 75
Estimated values

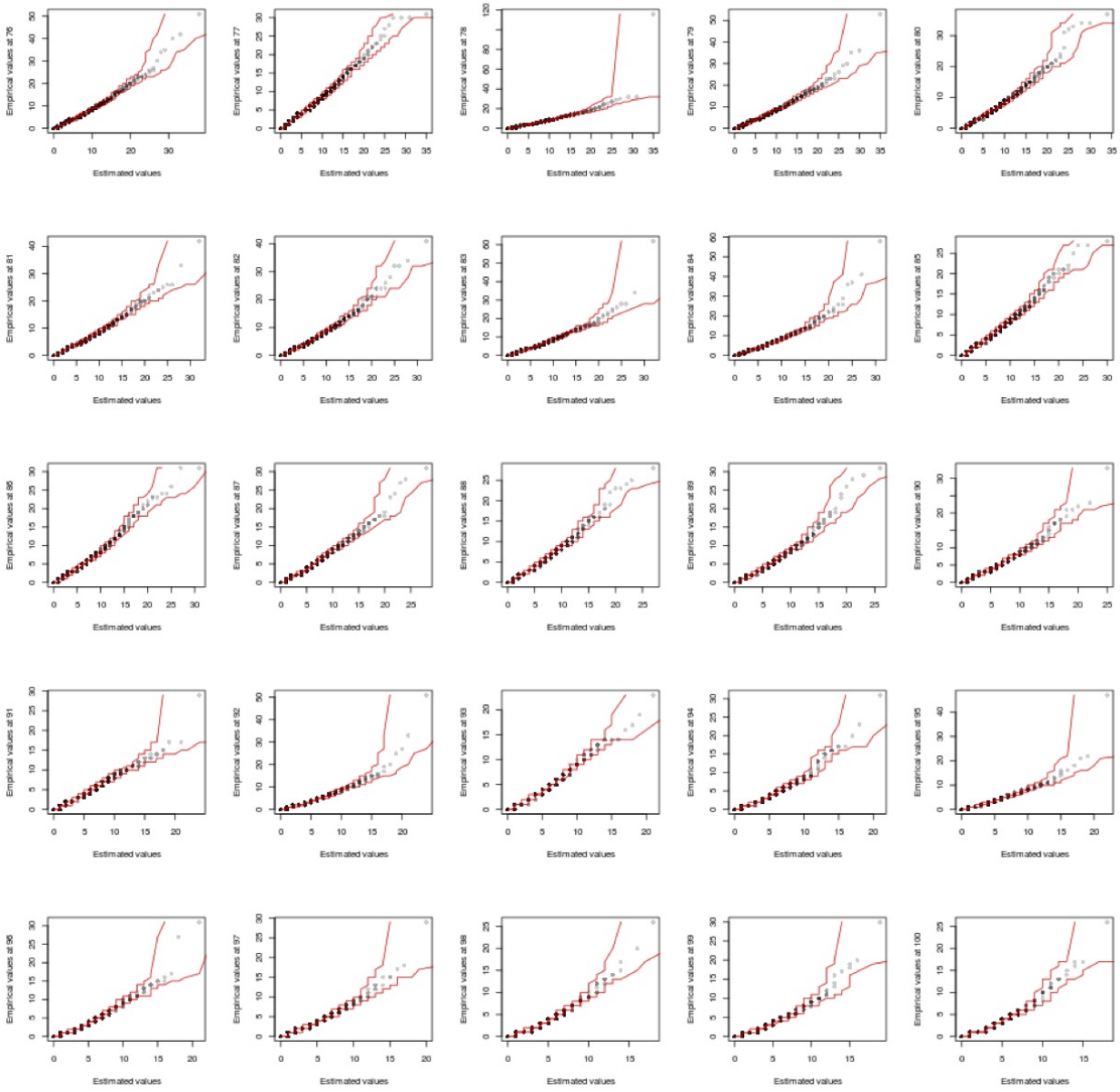
Empirical values at 76
Empirical values at 77
Empirical values at 78
Empirical values at 79
Empirical values at 80
Empirical values at 81
Empirical values at 82
Empirical values at 83
Empirical values at 84
Empirical values at 85
Empirical values at 86
Empirical values at 87
Empirical values at 88
Empirical values at 89
Empirical values at 90
Empirical values at 91
Empirical values at 92
Empirical values at 93
Empirical values at 94
Empirical values at 95
Empirical values at 96
Empirical values at 97
Empirical values at 98
Empirical values at 99
Empirical values at 100
Estimated values

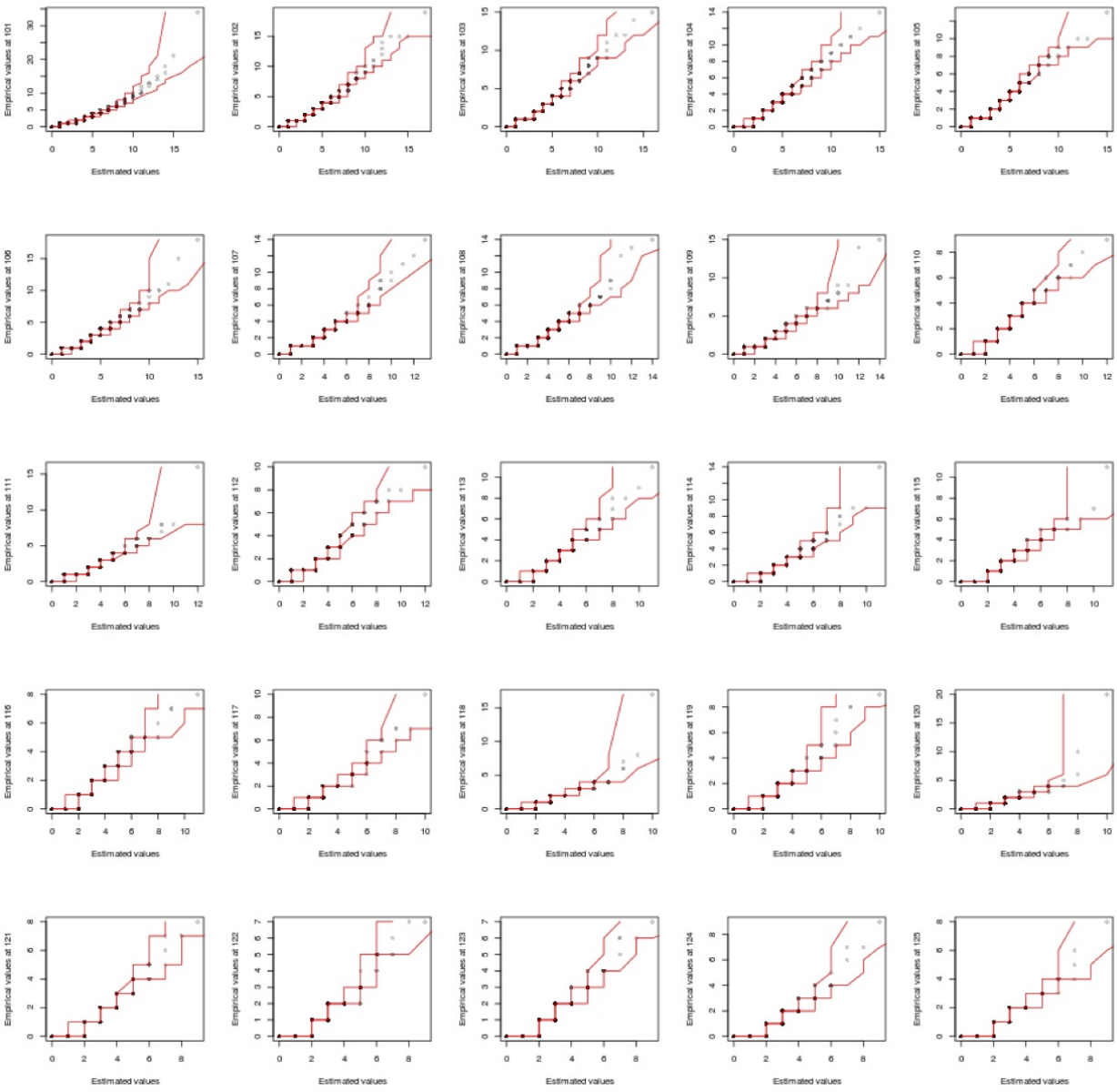
Empirical values at 101
Empirical values at 102
Empirical values at 103
Empirical values at 104
Empirical values at 105
Empirical values at 106
Empirical values at 107
Empirical values at 108
Empirical values at 109
Empirical values at 110
Empirical values at 111
Empirical values at 112
Empirical values at 113
Empirical values at 114
Empirical values at 115
Empirical values at 116
Empirical values at 117
Empirical values at 118
Empirical values at 119
Empirical values at 120
Empirical values at 121
Empirical values at 122
Empirical values at 123
Empirical values at 124
Empirical values at 125
Estimated values

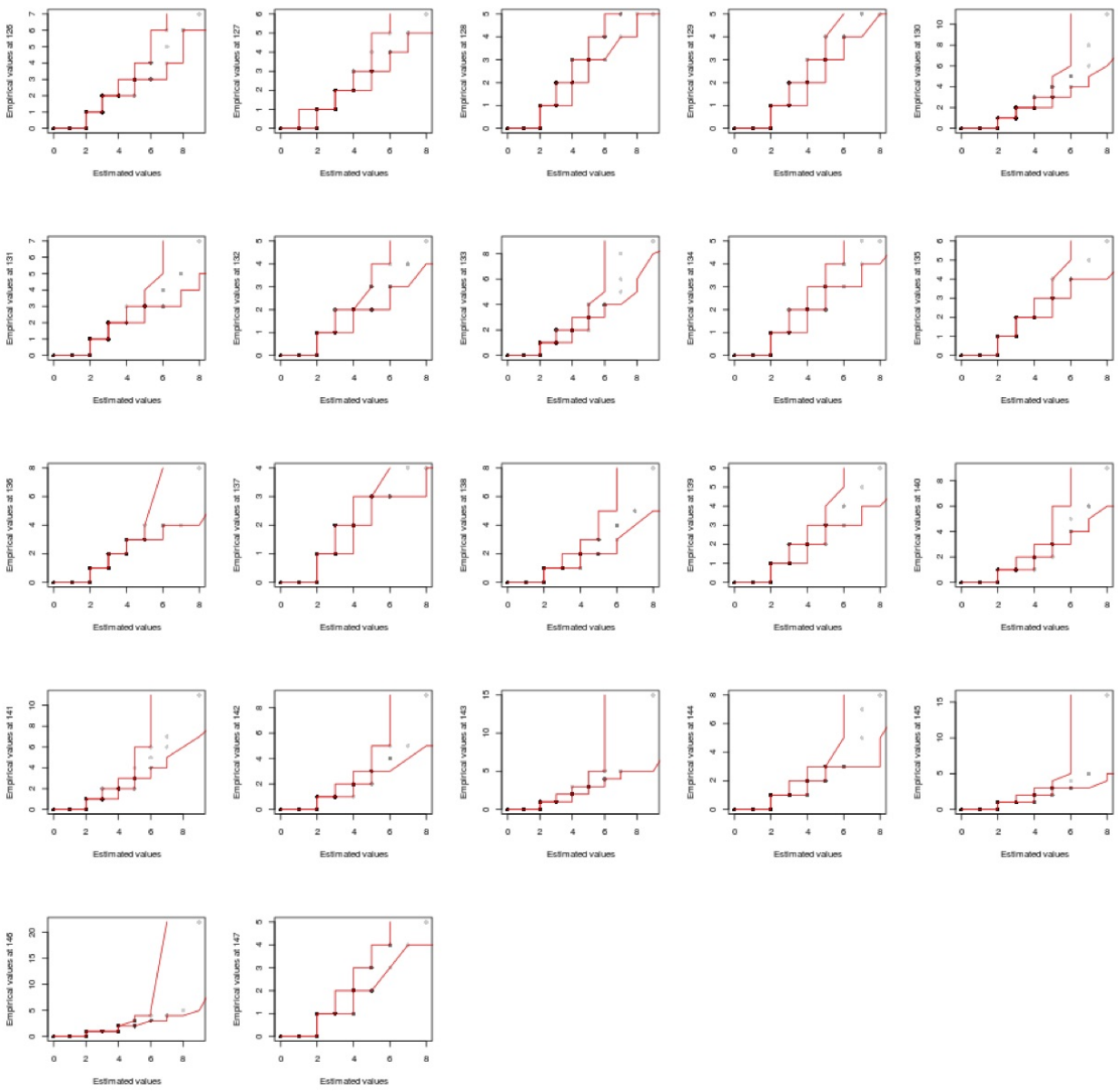

Figure S7: QQ-plots of negative binomial distributions for *nucleosomal fragment* midpoint counts of all 147 positions of nucleosome.

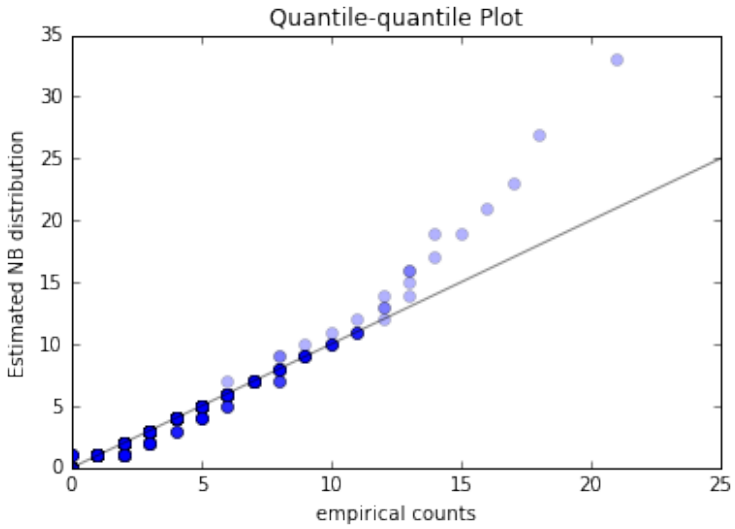

Figure S8: Quantile quantile plot of NB distribution of midpoint counts of *short factor fragments* to predict TF binding sites.

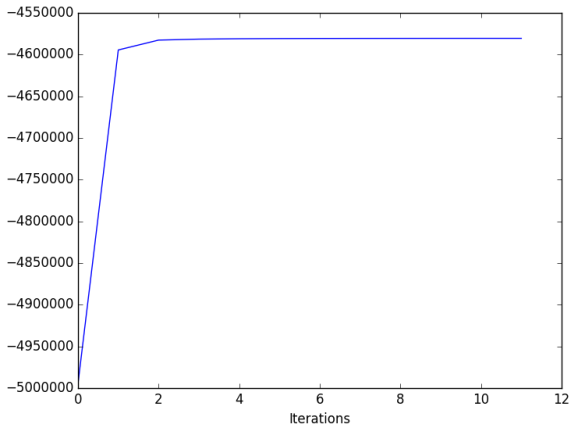

Figure S9: Likelihood in the 10 iterations of EM of RoboCOP.

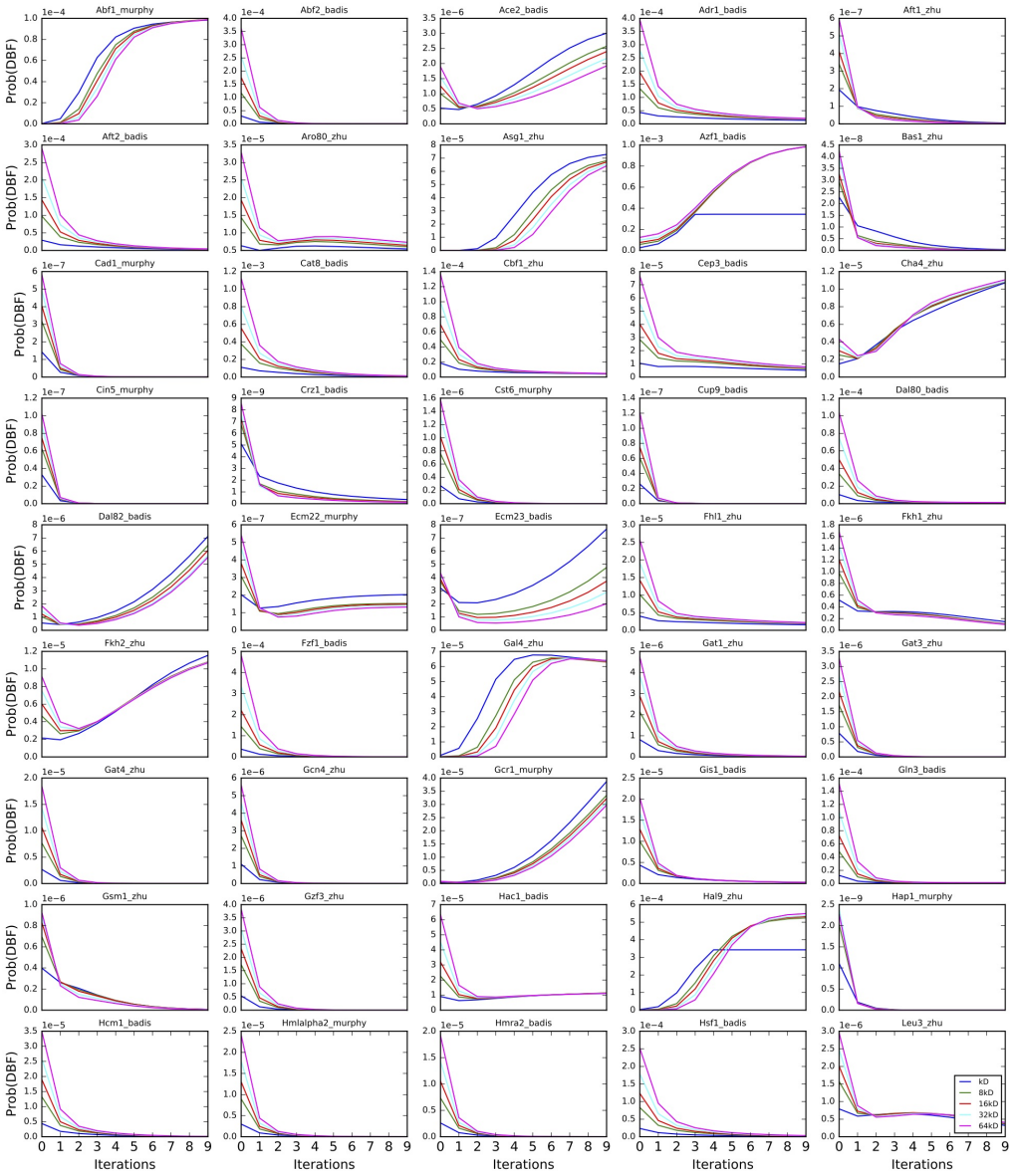
Abf1_murphy
Abf2_badis
Ace2_badis
Adr1_badis
Aft1_zhu
Aft2_badis
Aro80_zhu
Asg1_zhu
Azf1_badis
Bas1_zhu
Cad1_murphy
Cat8_badis
Cbf1_zhu
Cep3_badis
Cha4_zhu
Cin5_murphy
Crz1_badis
Cst6_murphy
Cup9_badis
Dal80_badis
Dal82_badis
Ecm22_murphy
Ecm23_badis
Fhl1_zhu
Fkh1_zhu
Fkh2_zhu
Fzf1_badis
Gal4_zhu
Gat1_zhu
Gat3_zhu
Gat4_zhu
Gcn4_zhu
Gcr1_murphy
Gis1_badis
Gln3_badis
Gsm1_zhu
Gzf3_zhu
Hac1_badis
Hal9_zhu
Hap1_murphy
Hcm1_badis
Hmlalpha2_murphy
Hmra2_badis
Hsf1_badis
Leu3_zhu
Prob(DBF)
Iterations
kD
8kD
16kD
32kD
64kD

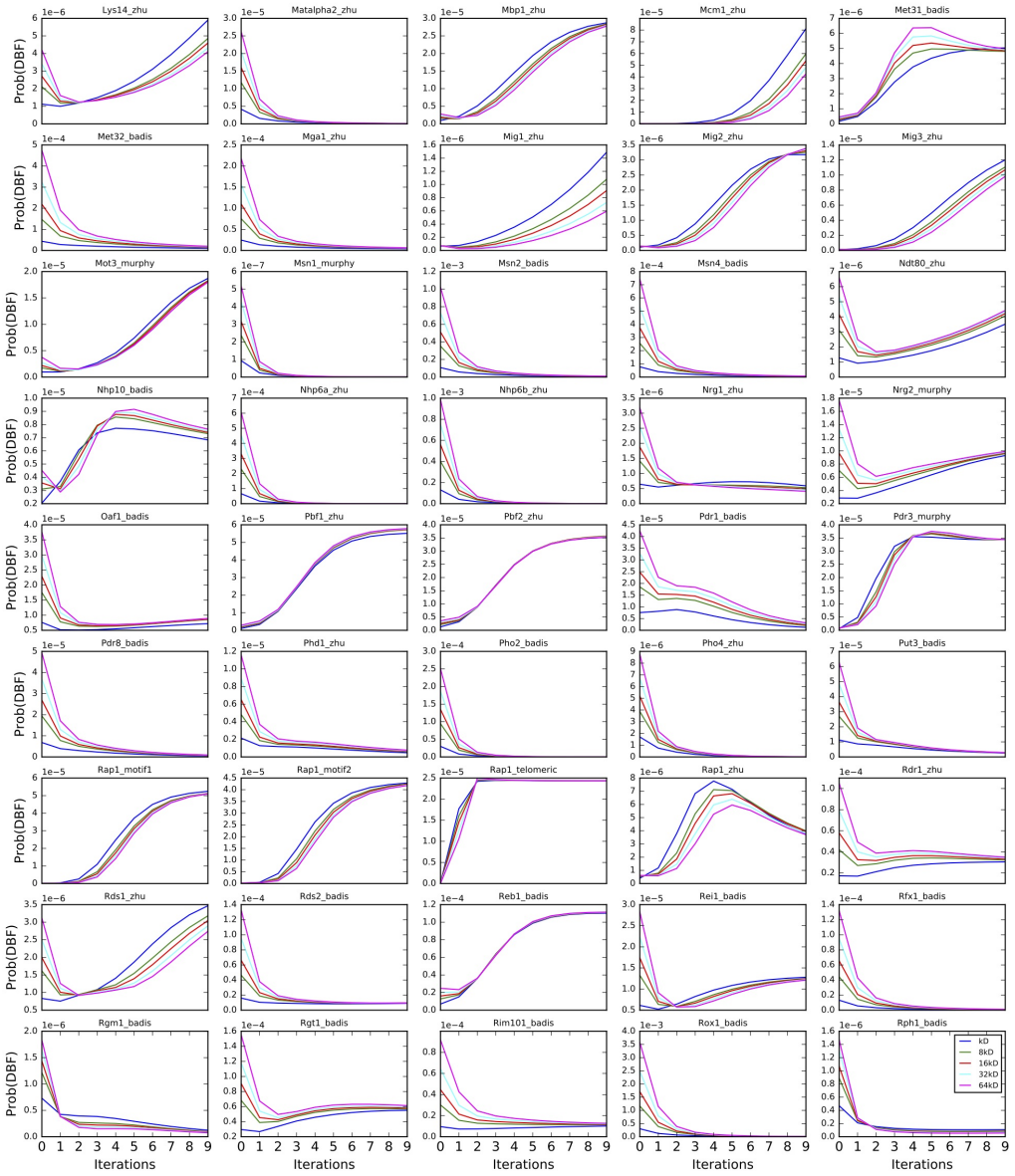
Lys14_zhu
Matalpha2_zhu
Mbp1_zhu
Mcm1_zhu
Met31_badis
Met32_badis
Mga1_zhu
Mig1_zhu
Mig2_zhu
Mig3_zhu
Mot3_murphy
Msn1_murphy
Msn2_badis
Msn4_badis
Ndt80_zhu
Nhp10_badis
Nhp6a_zhu
Nhp6b_zhu
Nrg1_zhu
Nrg2_murphy
Oaf1_badis
Pbf1_zhu
Pbf2_zhu
Pdr1_badis
Pdr3_murphy
Pdr8_badis
Phd1_zhu
Pho2_badis
Pho4_zhu
Put3_badis
Rap1_motif1
Rap1_motif2
Rap1_telomeric
Rap1_zhu
Rdr1_zhu
Rds1_zhu
Rds2_badis
Reb1_badis
Rei1_badis
Rfx1_badis
Rgm1_badis
Rgt1_badis
Rim101_badis
Rox1_badis
Rph1_badis
Prob(DBF)
Iterations
kD
8kD
16kD
32kD
64kD

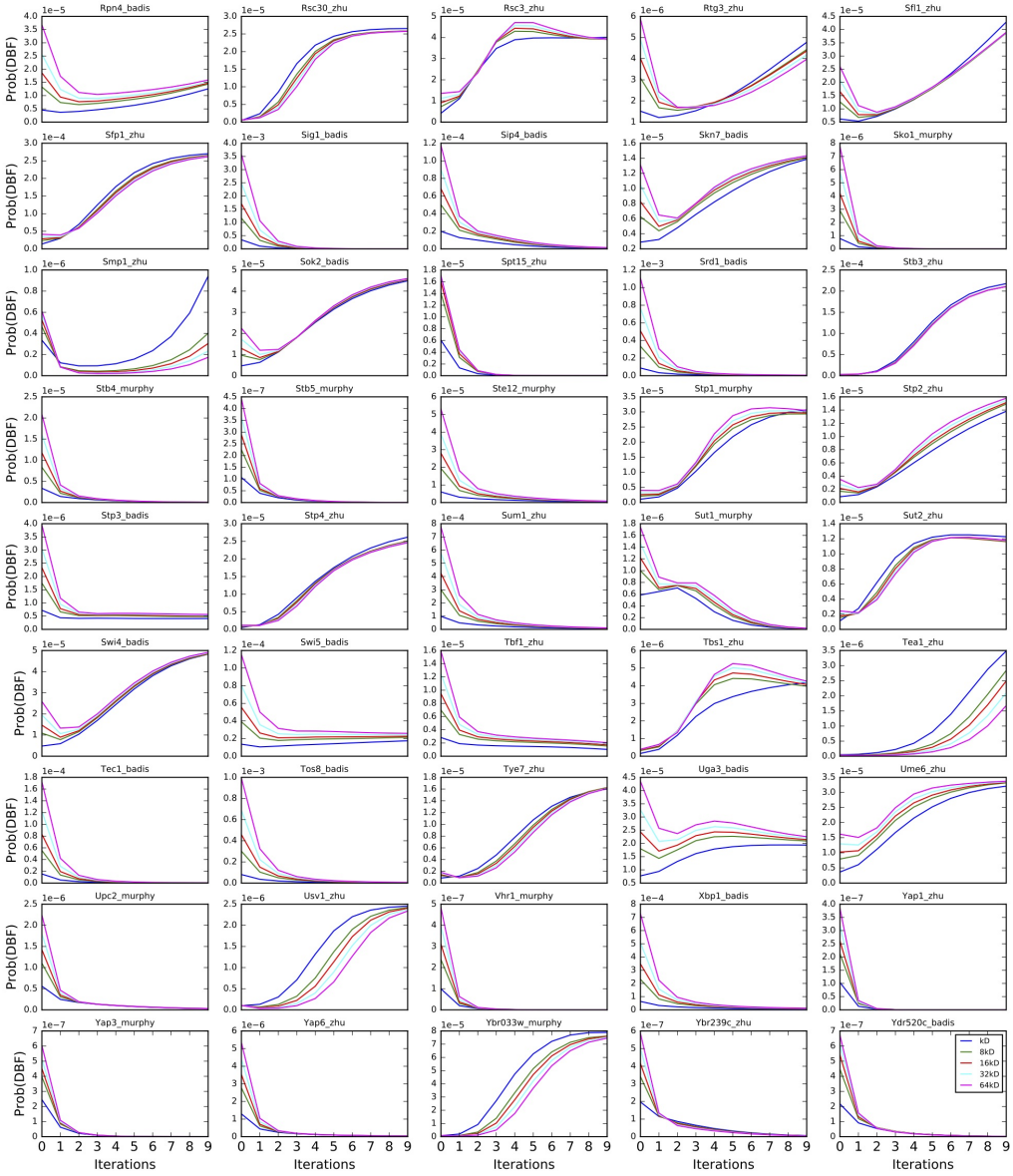
Rpn4_badis
Rsc30_zhu
Rsc3_zhu
Rtg3_zhu
Sfl1_zhu
Sfp1_zhu
Sig1_badis
Sip4_badis
Skn7_badis
Sko1_murphy
Smp1_zhu
Sok2_badis
Spt15_zhu
Srd1_badis
Stb3_zhu
Stb4_murphy
Stb5_murphy
Ste12_murphy
Stp1_murphy
Stp2_zhu
Stp3_badis
Stp4_zhu
Sum1_zhu
Sut1_murphy
Sut2_zhu
Swi4_badis
Swi5_badis
Tbf1_zhu
Tbs1_zhu
Tea1_zhu
Tec1_badis
Tos8_badis
Tye7_zhu
Uga3_badis
Ume6_zhu
Upc2_murphy
Usv1_zhu
Vhr1_murphy
Xbp1_badis
Yap1_zhu
Yap3_murphy
Yap6_zhu
Ybr033w_murphy
Ybr239c_zhu
Ydr520c_badis
Prob(DBF)
Iterations
kD
8kD
16kD
32kD
64kD

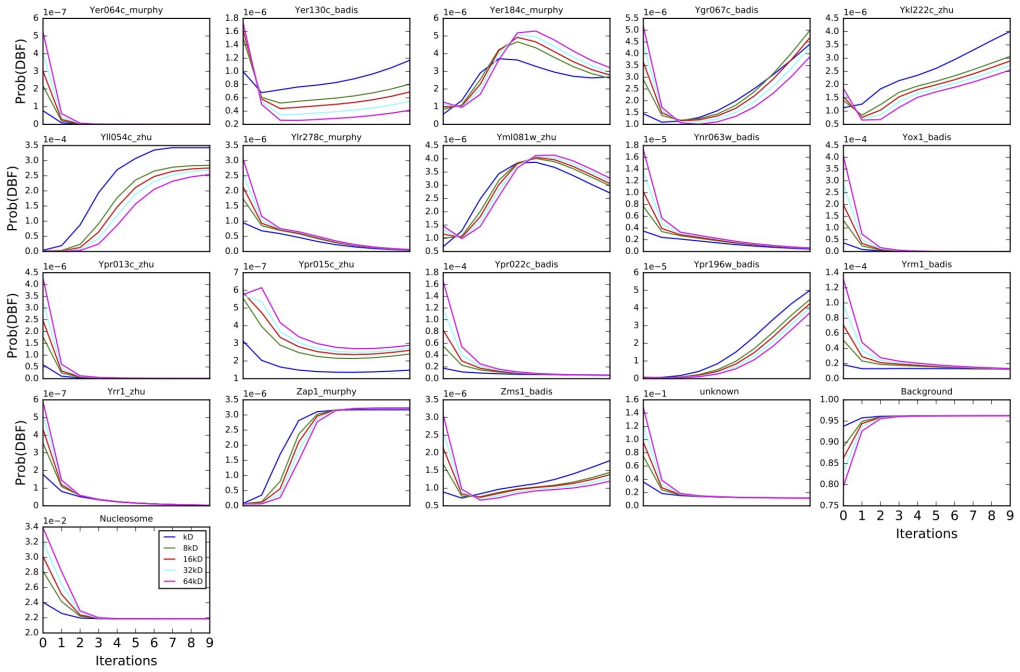

Figure S10: Transition weights of DBFs in every iteration of EM when for initializing using multiples of K_D.

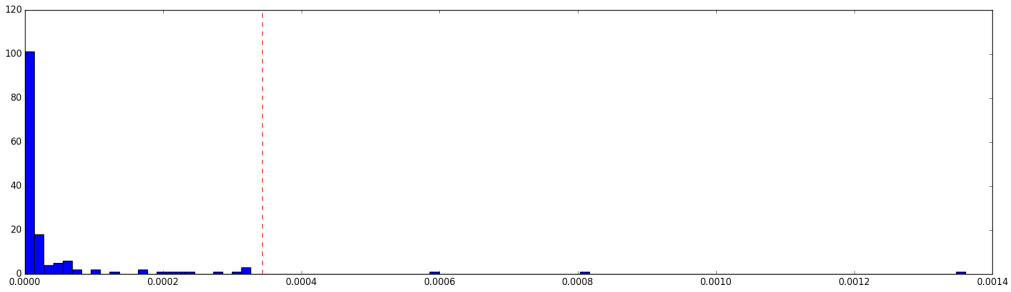

Figure S11: Choosing threshold for transition weight of TFs.

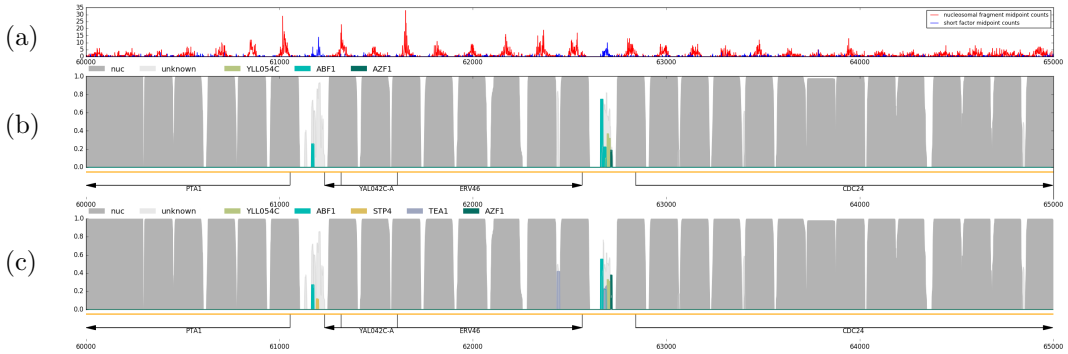

Figure S12: (a) MNase-seq fragment midpoint counts. Running RoboCOP (b) with and (c) without threshold cutoff of TF weights. In (c) we see more clustering of TFs means there are more false positives. RoboCOP gives fewer false positives when TF transition weights are updated with threshold.

References

Harbison, C. T., Gordon, D. B., Lee, T. I., Rinaldi, N. J., MacIsaac, K. D., Danford, T. W., Hannett, N. M., Tagne, J.-B., Reynolds, D. B., Yoo, J., Jennings, E. G., Zeitlinger, J., Pokholok, D. K., Kellis, M., Rolfe, P. A., Takusagawa, K. T., Lander, E. S., Gifford, D. K., Fraenkel, E., and Young, R. A. (2004). Transcriptional regulatory code of a eukaryotic genome. *Nature*, **431**(7004), 99–104.

Kasinathan, S., Orsi, G. A., Zentner, G. E., Ahmad, K., and Henikoff, S. (2014). High-resolution mapping of transcription factor binding sites on native chromatin. *Nature Publishing Group*, **11**(2), 203–209.

MacIsaac, K. D., Wang, T., Gordon, D. B., Gifford, D. K., Stormo, G. D., and Fraenkel, E. (2006). An improved map of conserved regulatory sites for Saccharomyces cerevisiae. *BMC Bioinformatics*, **7**(1), 113.

Rhee, H. S. and Pugh, B. F. (2011). Comprehensive genome-wide protein-DNA interactions detected at single-nucleotide resolution. *Cell*, **147**(6), 1408–1419.